Supporting information available

Structural information on our SBA-15 samples

TEM micrographs of a crystallite of our powdered SBA-15 sample are presented in fig. 1s

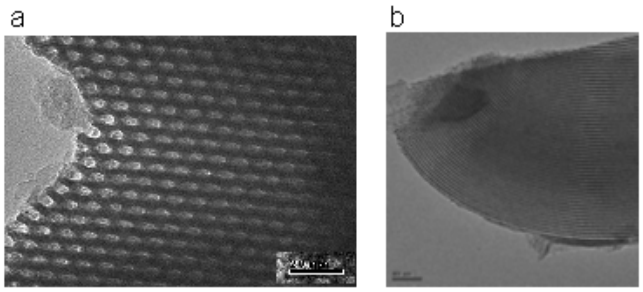

Figure 1s

The exchange model

A comparison between the two- and four-site exchange models was conducted in order to find the region where the two models are about equal. As mentioned in the text, two parameters were used in the comparison, namely, FWHH of the centerband of ^{2}H MAS spectra, and the ratio between the intensities of the first sideband (I_1) and centerband (I_o). Contour plots of this ratio, for the two- and four-site exchange models as a function of $\{\log(k_{bf}),P_b\}$ are presented in fig. 2s.

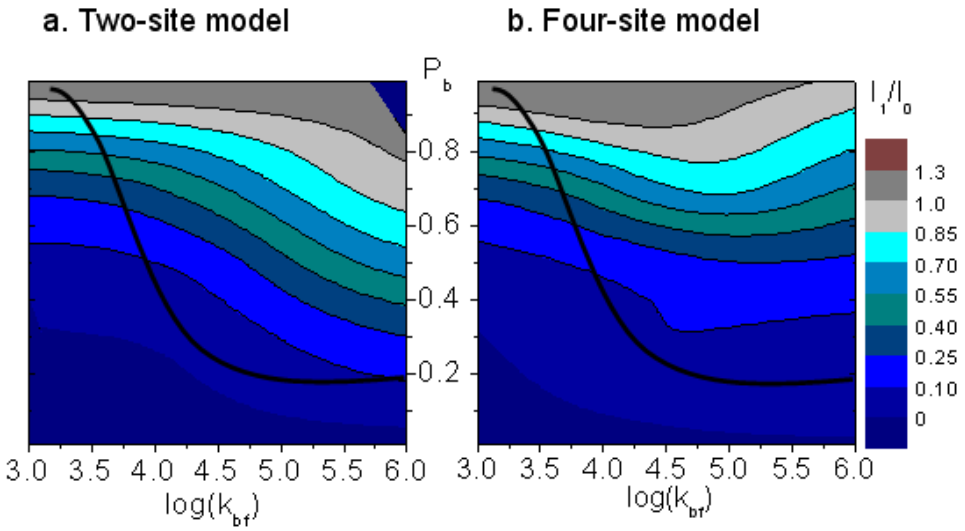

Figure 2s

Fig. 3s presents the intensity ratio (I_1/I_0) of ^{2}H sideband spectra versus P_b for $k_{bf} = 10^3$ s^{-1} (triangles) and $k_{bf} = 3.2 \cdot 10^5$ s^{-1}(circles) derived from simulated spectra, using the two-site (filled) and four-site (empty), with $\theta = 90^0$,exchange model with $\nu_Q = 51$ kHz and $\nu_r = 6$ kHz. The equivalence between the ratios for $k_{bf} = 10^3 s^{-1}$ is clearly observed.

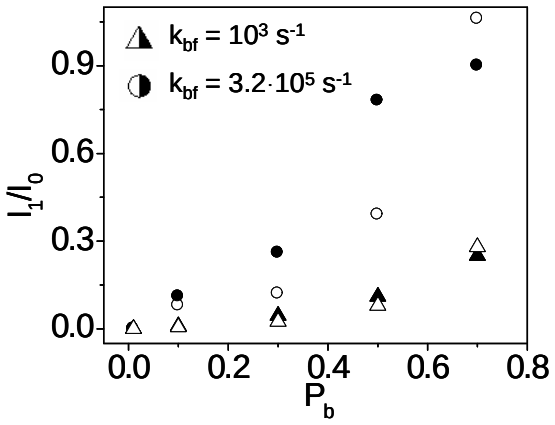

Figure 3s

The degree of precision, of the two-site exchange model, is demonstrated in the contour plot in fig. 4s. The contour plot presents the data points of our measurements. The horizontal and vertical width of these points indicate the degree of accuracy of the two-site exchange model. As can be seen, the majority of the data points in our experiments fall under the black line.

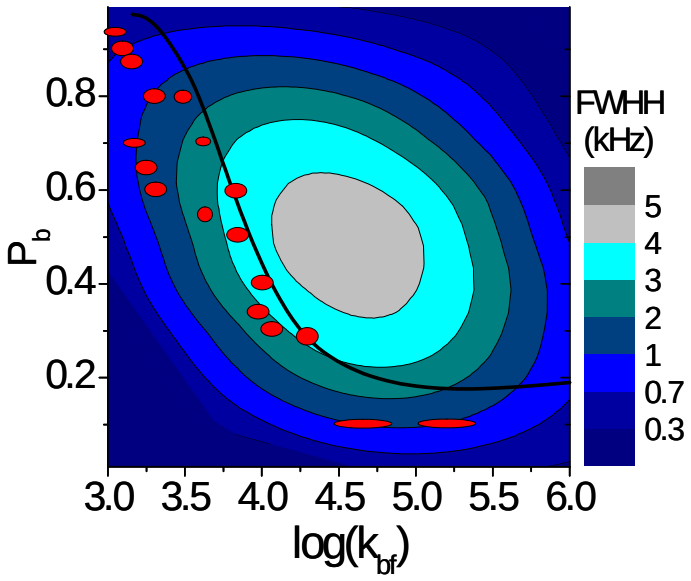

Figure 4s

In the case the dynamic parameters $\{k_{bf}$,$P_b\}$ fall outside the overlapping region in fig. 4 of the main text, we must repeat the whole line fitting procedure, using a four-site exchange model. This procedure is not straightforward due to the angle-θ dependence. A contour plot of the FWHH of the centerband of ^{2}H MAS spectra for $\theta = \pi/4$ as a function of $\log(k_{bf})$ and P_b for $\nu_Q = 51\ kHz$ and $\nu_r = 6\ kHz$ has been calculated and is presented in fig. 5s. The spectra on both sides are calculated for $k_{bf} = 10^3$ and $3.2 \cdot 10^5 s^{-1}$ for P_b values given on the left. Again the area below the solid line is independent of θ.

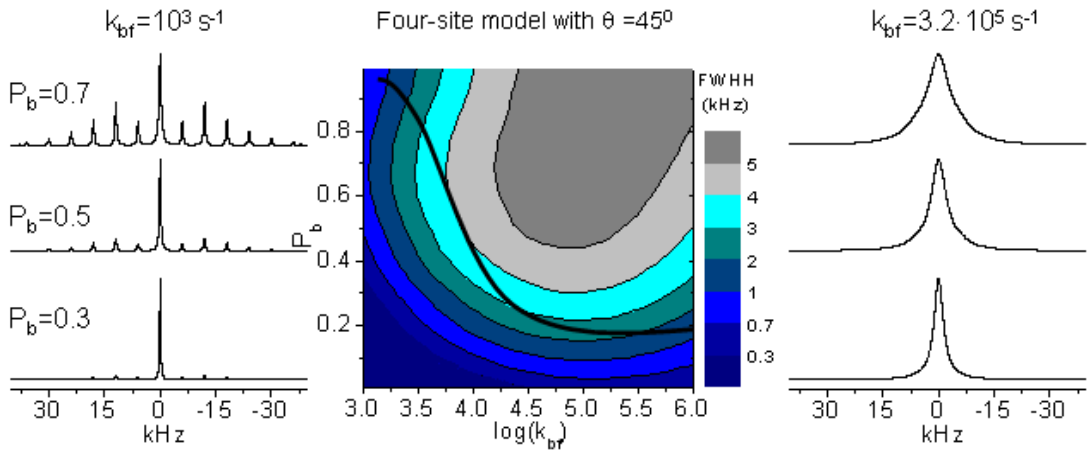

Figure 5s

To demonstrate the sensitivity of the dynamic MAS spectra to changes in the quadrupole coupling constant and spinning frequencies an additional contour for $\nu_Q = 160\ kHz$ and $\nu_r = 10\ kHz$ is calculated and shown in fig. 6s. This quadrupole frequency corresponds to a CD group in an exchanging organic molecule. The spectra on both sides are simulated with $k_{bf} = 10^3$and $3.2 \cdot 10^5\ s^{-1}$ and for P_b values given on the left.

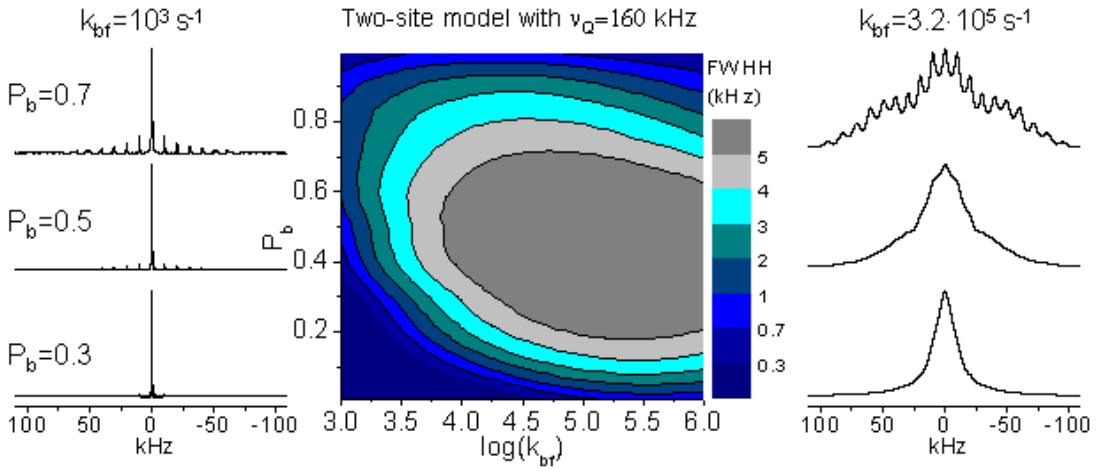

Figure 6s

A spectral feature of all MAS sideband spectra of these two- and four-site exchange models is the appearance of an intense centerband at k_{bf} values below $10^4\ s^{-1}$. This feature is characteristic for an exchange process with one isotropic site. Other exchange models will not exhibit a dominant centerband at a wide range of rate constants. For example, when all four sites have equally populated non-zero effective quadrupole tensors, while their frequencies and orientations average to zero in the fast exchange limit, their dynamic spectra do not show any strong centerband intensity. A set of simulated spectra for such a case is presented in fig. 7s with $\nu_Q = 51\ kHz$ and $\nu_r = 6\ kHz$.

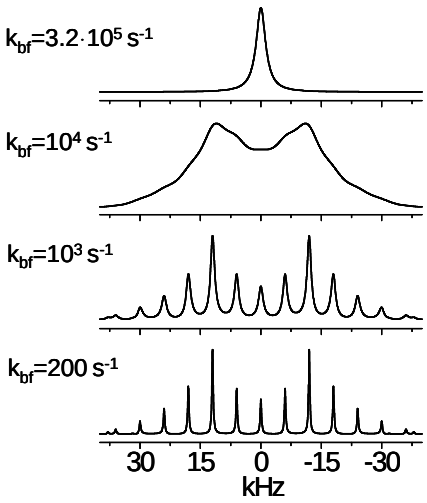

Figure 7s

Our spectra could be a superposition of a set of spectra with a distribution of values for the

parameters $\{k_{bf}, P_b\}$. However, from our best-fit spectral analysis using the two-site model we determine only average rate constants, k_{bf}, and relative populations, P_b. The deviations between spectra that are simulated, based on average parameters $\{k_{bf}, P_b\}$ and based on a summation of a distribution of spectra with different parameters, depend on the actual deviations of these parameters. To demonstrate this we show here (fig. 8s) a comparison between dynamic ^{2}H spectra calculated using a single pair of parameters $\{k_{bf}, P_b\}$ and a distribution of parameters. We chose to fit the ^{2}H MAS spectrum at $p = 11$ of the alanine-d_3 in SBA-15, using the following parameters: for the solid line $k_{bf} = 4.5 \cdot 10^3 s^{-1}$, $P_b = 0.7$, and for the dotted line a combination of 20% $k_{bf} = 1 \cdot 10^3 s^{-1}$, $P_b = 0.99$, 40% $k_{bf} = 20 \cdot 10^3 s^{-1}$, $P_b = 0.3$, and 40% $k_{bf} = 5.5 \cdot 10^3 s^{-1}$, $P_b = 0.7$.

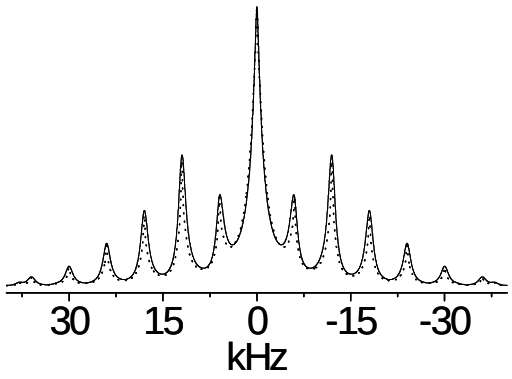

Figure 8s

Alanine-d_3 inside SBA-15

^{29}Si NMR spectrum was measured (and shown in fig. 9s), and analyzed in terms of the relative intensities of the Q^3 line at -100 *ppm* and of the Q^4 line at -110 *ppm*. The ratio between the two integrated intensities of these lines is 3 : 7. Combining this ratio with the pore volume and diameter, obtained from the N_2 adsorption measurements (summarized in table 1 in the text), we find that the estimated number of hydroxyl groups per nm^2 is about 3.5.

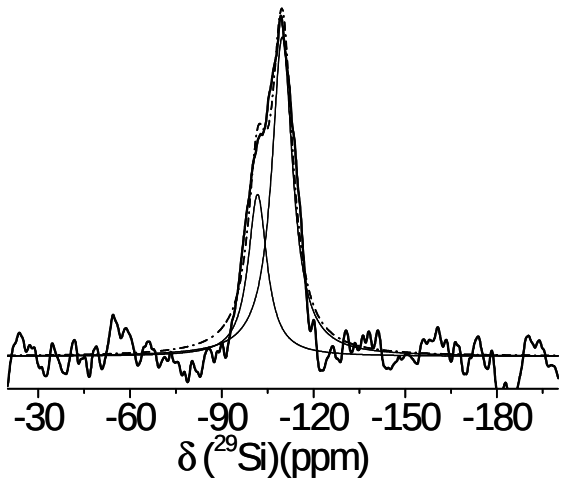

Figure 9s

The histogram in fig. 10s presents a possible cluster size distribution $d(p,x)$ of the protons in the inner surface of SBA-15 , *i.e*, the relative number of oxygen sites occupied by x protons for each p value. $p=4$ (solid), $p=6$ (sparse), $p=11$ (dense).

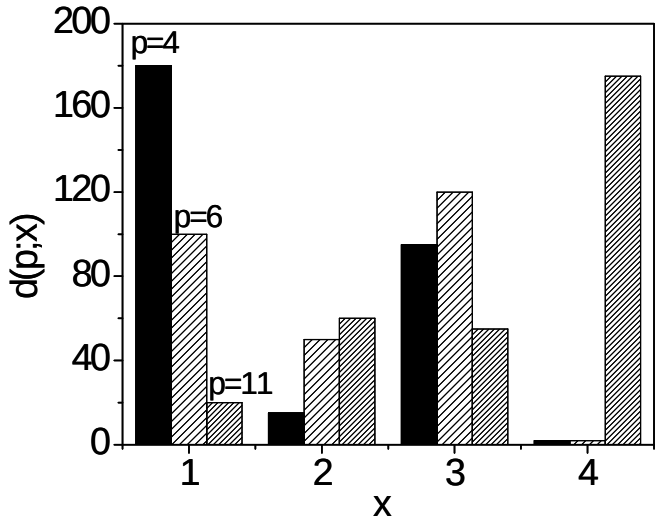

Figure 10s

Fig. 11s presents the total integrated intensity (full circles) of ^{1}H spectra of a sample of SBA-15 loaded with alanine-d_3, with $p=12$ (a) and 20 (b) at different temperatures, with the relevant spectra on the right. The intensity of the main components of the spectra between $\sim (3.8-5)$ *ppm* are also drawn in the figure by open circles. The rest of the intensity is mainly due to the line around $\sim (6.8-7)$ *ppm*.

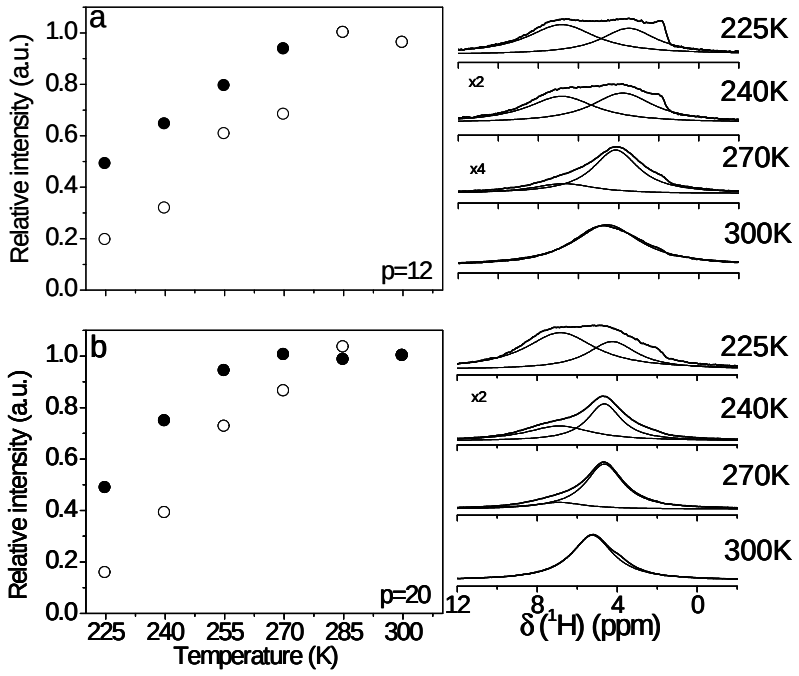

Figure 11s

Fig. 12s presents the ^{2}H MAS spectra of a sample of alanine-d_3 inside SBA-15 with $p = 20$ at different temperatures. In (a) the experimental spectra are shown. These spectra were decomposed into narrow and broad components. The broad component is presented in (b) and in (c) their best-fit simulated spectra are drawn. The resulting dynamic parameters of the fitting procedure are at 300K:($k_{bf} = 160 \cdot 10^3 s^{-1}$, $P_b = 0.1$), at 285K: ($k_{bf} = 10 \cdot 10^3 s^{-1}$, $P_b = 0.4$), at 270K: ($k_{bf} = 7 \cdot 10^3 s^{-1}$, $P_b = 0.5$), at 255K: ($k_{bf} = 2 \cdot 10^3 s^{-1}$, $P_b = 0.8$), at 240K: ($k_{bf} = 1 \cdot 10^3 s^{-1}$, $P_b = 0.9$) and at 225K: ($k_{bf} = 0.3 \cdot 10^3 s^{-1}$, $P_b = 0.99$).

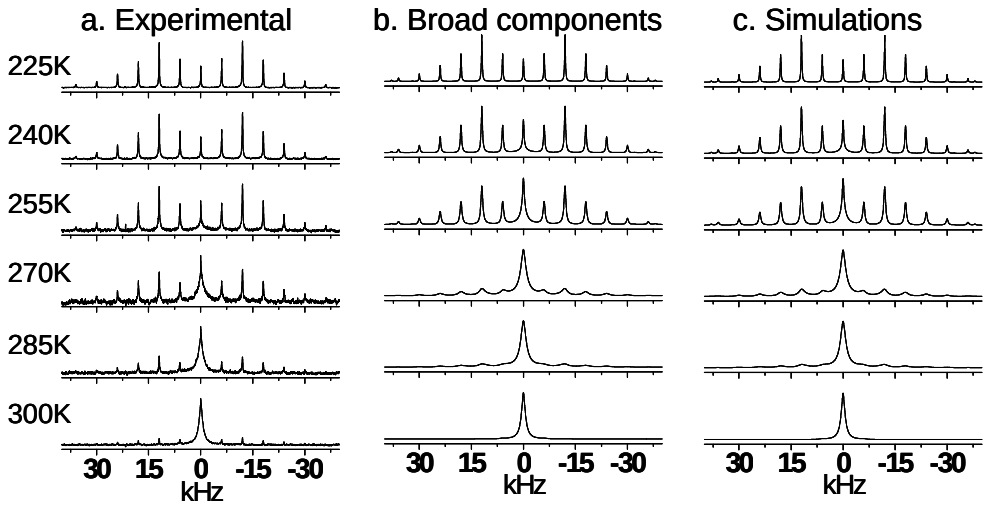

Figure 12s

This information is available free of charge via the Internet at http://pubs.acs.org.